Int. J. Microgravity Sci. Appl., 36 (4) (2019) 360402
DOI: 10.15011//jasma.36.360402

IIII Original Paper IIII

Behavior of Subcooling Jet Injected into a Bulk Liquid in a Tank under Normal- and Micro-gravity Conditions

Osamu KAWANAMI [1], KentaroTAKEDA [1], Ryoma NAGUCHI [1], Ryoji IMAI [2], Yutaka UMEMURA [3], Takehiro HIMENO [4]

Abstract

In the future exploration for deep space, cryogenic fluid will be used as propellant and oxidizer for spacecraft. The increasing of tank pressure is caused by boil off gas (BOG) induced by heat leakage into the tank from the surrounding environment. Reducing of BOG is derived from destroy of thermal stratification of a bulk liquid in the tank. Therefore, development of Thermodynamic Vent System (TVS) for the purpose of prevent of loss of cryogenics propellant in future space system is needed. TVS combining jet mixing, spray, and heat spot removal by forced cooling using Electro-hydro-dynamics is under consideration by authors. Destroying thermal stratification without venting by using subcooling mixing jet will be developed for a key technology of TVS. In this paper, the behavior of the mixing jet by visualization method and description about the motion of the jet with a simple one-dimensional model without heat transfer is reported. In our simple dynamic model, a single sphere droplet as the tip of the jet is assumed and an equation of the motion is applied for the droplet. The results of analysis model and experimental data taken by shadowgraph system are compared. In addition, microgravity experiment is performed, and flow behavior in microgravity is described.

Keyword(s): Jet mixing, Visualization, Dynamic analysis model, Microgravity
Received 30 August 2019, accepted 22 October 2019, published 31 October 2019

1. Introduction

For the future space transport system, the improvement of the performance of the propulsion systems is required to increase the payload weight. In order to achieve long-term space exploration for the future space activity planning, thermal management technology for a cryogenic propellant storage tank is an important issue [1–3]. The cryogenic propellant storage tank suffers loss of the propellant due to boil-off, that is induced by heat leakage into the tank from the surrounding environment. To control the tank pressure within its structural limitation, the boil-off gas (BOG) should be released from the tank to the space. Schaffer and Wenne analyzed that the boil-off rate considerably influenced the payload weight in long-term missions to explore Mars [4].

Concept of the zero boil-off (ZBO) and/or reduced boil-off (RBO) researched by NASA Glenn Research Center [5–7] has developed as a pressure control method of cryogenic storage tank by synergistic application of passive insulation [8], active heat removal [9,10], and forced mixing within the tank [11]. They published many reports about ZBO/RBO studies [12–15] including the experiment in space [16].

Authors started the researches about Thermodynamic Vent System (TVS) [17,18], which is a method of destroying the thermal stratification by mixing subcooling jet supplied from the bottom of the tank as shown in **Fig. 1**. In addition, TVS combining jet mixing, spray, and heat spot removal by forced cooling based on Electro-hydro-dynamics is under consideration. Imai *et al.* reported the numerical analysis and verification ground test using liquid nitrogen about the destruction of thermal stratification by jet mixing [19].

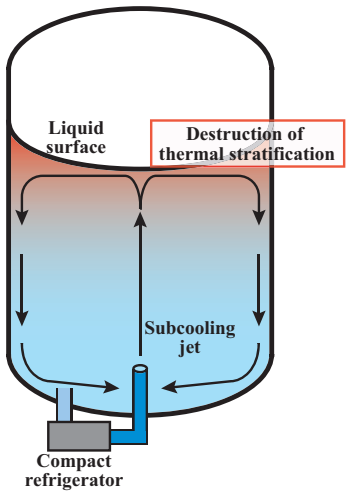

Fig. 1 Concept of subcooling jet mixing for thermodynamic vent system.

1 Department of Mechanical Engineering, University of Hyogo, 2167 Shosha, Himeji, Hyogo 671-2280, Japan.
2 Department of Engineering, Muroran Institute of Technology, 27-1 Mizumoto-cho, Muroran, Hokkaido 050-8585, Japan.
3 Japan Aerospace Exploration Agency, 2-1-1 Sengen, Tsukuba, Ibaraki 305-8505, Japan.
4 Department of Aeronautics and Astronautics, University of Tokyo, 7-3-1 Hongo, Bunkyo-ku, Tokyo 113-8656, Japan.
(E-mail: kawanami@eng.u-hyogo.ac.jp)

© 2019 The Jpn. Soc. Microgravity Appl. http://www.jasma.info/journal/

About the jet mixing of the liquid in the tank, CFD simulations [19–22] have been reported. Regarding jet mixing experiments in microgravity, few numbers of experiments have been conducted by Aydelott [18]. He reported the results from the axial-jet mixing of ethanol in 10-cm-diameter containers under zero-, reduced-, and normal-gravity conditions, and identified the four distinct jet flow patterns in microgravity; (1) dissipation of the liquid jet in the bulk-liquid region, (2) geyser formation, (3) collection of the jet liquid in the aft end of the tank, (4) liquid circulation over the aft end of the tank and down the tank wall. To destroy of thermal stratification by mixing jet, it is important that the jet reaches the liquid surface at least as shown in **Fig. 1** (pattern (1)) or pattern (4). However, there were not experimental reports about direct observation of subcooling jet behavior in a bulk liquid for above-mentioned purposes.

Therefore, our study is focusing on the relationship between the behavior of the subcooling jet injected into the bulk liquid in the tank and the mixing effect to destroy of thermal stratification. Here, we report to illustrate the behavior of the mixing jet by visualization method and to attempt description about the motion of the jet with a simple one-dimensional model without heat transfer.

Nomenclature

C_D :	drag coefficient	[-]
Re :	Reynolds number	[-]
F_r :	resistance force	[N]
F_i :	inertia resistance force	[N]
F_v :	viscous drag	[N]
F_g :	gravitational force	[N]
v :	velocity	[m/s]
t :	time	[sec]
T :	temperature	[°C]
ΔT :	temperature difference	[K]
d :	diameter of droplet assuming the tip of jet	[m]
V :	volume of the droplet	[m^3]
S :	cross section area of the droplet	[m^2]
m :	mass of the droplet	[kg]
H_l :	liquid height in the tank	[m]
$\dot{m}_j$:	flow rate of subcooling jet	[mL/min]
ρ :	density	[kg/m^3]
μ :	viscosity	[Pa·s]

Subscripts

b :	bulk liquid in the tank
j :	jet
0 :	initial condition

2. Experiment

2.1 Experimental apparatus

Figure 2 shows the experimental apparatus used in this study. The main components of the apparatus are a pump (GA-V21.J8FS.A, Micropump), a Coriolis flow meter (FD-SS02A, Keyence Co.), a reservoir tank for subcooling jet, a test tank, pressure sensor (AP-C30, Keyence Co.) and thermocouples. The test tank is made by SUS306, and the dimensions of the tank inside are 150 mm in height × 75 mm in width × 26 mm in depth, so the volume of the tank is 292.5 mL. For the observation the flow behavior inside the tank, the quartz glass window is set at the both sides of the tank. Four ceramic heaters are installed on each side wall of the tank to warm-up for liquid in the tank. In order to measure the temperature distribution along the axial direction inside the tank, two groups with eight thermocouples which have a diameter of 1.0 mm are arranged near the center of the tank and near the wall. The interval between each thermocouple in line is 20 mm.

The jet nozzle is located at the center of the tank bottom. The nozzle shape is a circular tube with an inner diameter of 0.5 mm and an outer diameter of 1.56 mm, and it is projected 13 mm-upward from the bottom of the tank.

There are two types of observation systems, the shadowgraph and high-speed camera system for ground experiments and back-light and CCD system for microgravity experiments. The field of view of the shadowgraph and high-speed camera system (SS50 and k8-USB, KATOKOKEN Co. Ltd.) is 48 mm in diameter, and the frame rate of high-speed camera is set at 1,000 fps. The frame rate of the CCD camera (IK-CU44/IK-C44H, Toshiba Co. Ltd.) is 30 fps.

Temperature data and pressure data are collected using a data logger (LR8400/LR8501, HIOKI E.E. Co.) with a measurement rate of 100 Hz.

FC-72 which is a kind of Fluorinert produced by 3M, is used as a test fluid.

2.2 Experimental procedure and conditions

Experimental parameters are liquid height in the test tank H_l, flow rate of subcooling jet $\dot{m}_j$, subcooling jet temperature T_j and bulk liquid temperature in the tank T_b. Firstly, the liquid height in the tank H_l is set, and the liquid is heated by a ceramic heater up to the target temperature. After T_b reaches the target temperature, we turn off the heater power and wait until the temperature difference in the axial direction of the liquid in the test tank is nearly constant. The reservoir tank for subcooling jet neither heating nor cooling, so subcooling jet temperature T_j is kept around the ambient temperature. Therefore, temperature difference between subcooling jet and bulk liquid in the test tank depends on heating power of ceramic heaters. Under the steady state of the temperature field in the bulk liquid, subcooling jet is injected into the bulk liquid during 2 seconds.

Microgravity experiments are conducted in a drop-tower, COS-

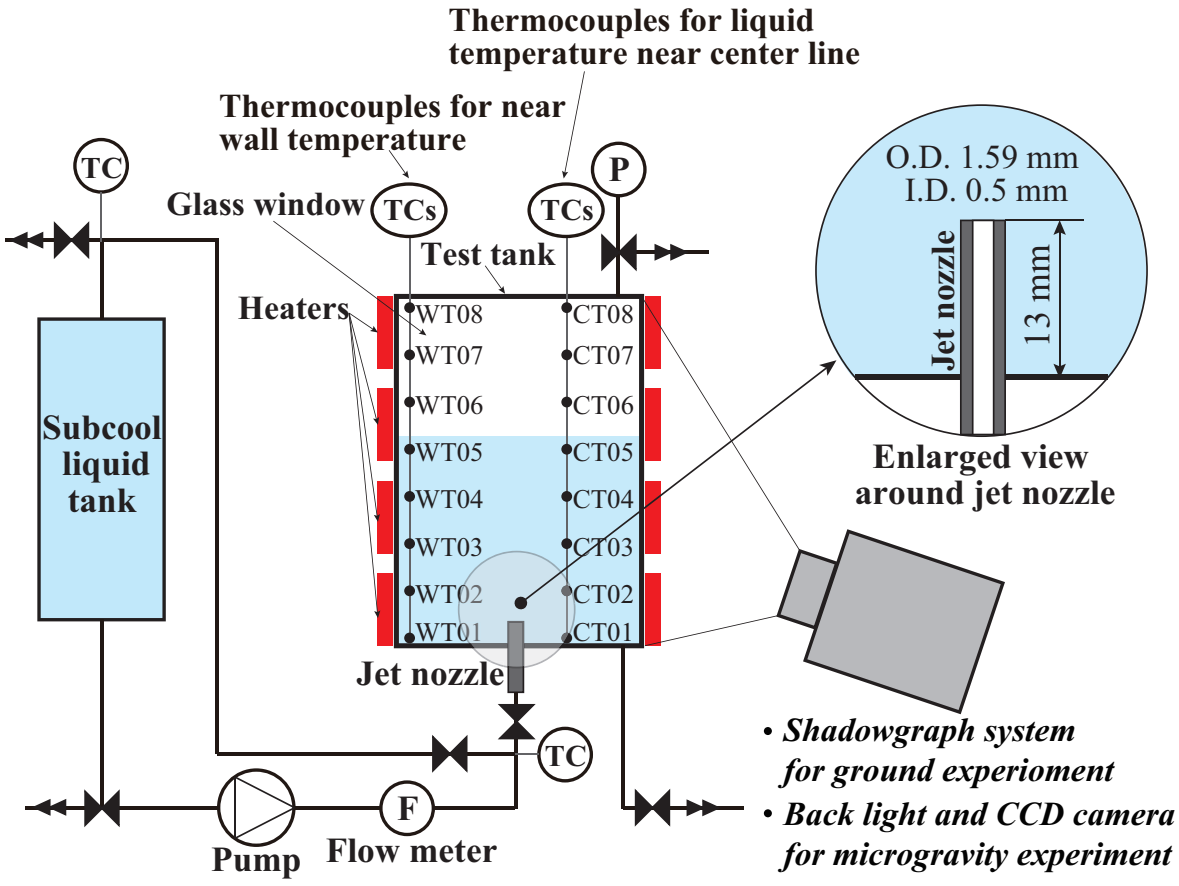

Fig. 2 An experimental set-up.

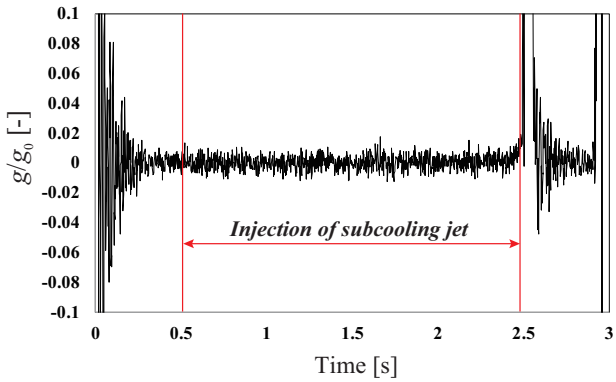

Fig. 3 As an example of gravitational acceleration data. The capsule dropped at $t = 0$ sec, and the subcooling jet is injected for 2 seconds after 0.5 seconds from the capsule dropped.

MOTORRE, operated by Uematsu Electric Co., Ltd. COSMOTORRE has 50 m in height, and its microgravity period and level are about 2.5∼3 seconds and $10^{-2} \sim 10^{-3}$ G. In the microgravity experiment, the subcooling jet is injected for 2 seconds after 0.5 seconds from the capsule dropped, as shown in **Fig.3**.

In this study, the range of experimental parameters are set as follows; $H_l = 75 \sim 100$ mm, $\dot{m}_j = 5 \sim 110$ mL/min, $T_j = 5 \sim 20$ °C and $T_b = 30 \sim 45$ °C.

3. Simple dynamics model for subcooling jet

In order to estimate the motion of the tip of the subcooling jet injected into the bulk liquid, one-dimensional simple dynamic analysis is discussed. Here we assume a single sphere droplet as the tip of the jet and an equation of the motion is applied for the droplet. In the case of the subcooling droplet pushing from the jet nozzle into the liquid in the tank as shown in **Fig. 4**, the motion of the droplet can be expressed by the following equation;

$$m\frac{dv}{dt} = -F_r - F_g, \tag{1}$$

where m, v, t, F_r and F_g are mass of the droplet, velocity of the droplet, time, resistance force applied to droplets from the surrounding fluid, and gravitational force, respectively.

F_r is switched to inertial resistance F_i and viscous resistance F_v depending with $Re = \rho_j v d/\mu_j$ as a function of the droplet velocity v,

$$F_r = \begin{cases} F_i = C_D \frac{(\rho_j - \rho_b) S v^2}{2} & \text{for } Re > 1, \\ F_v = 3\pi\mu d v & \text{for } Re < 1, \end{cases} \tag{2}$$

where C_D, S and d are drag coefficient, cross section area, $\pi d^2/4$,

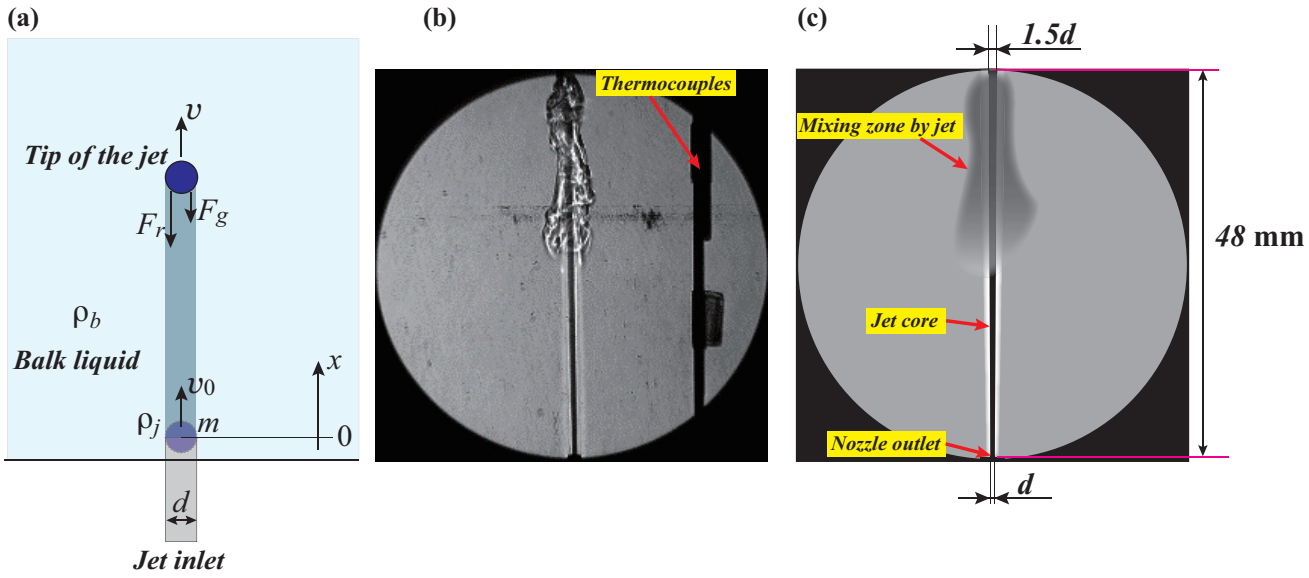

Fig. 4 The simple model for jet motion. (a) A droplet model assuming the tip of subcooling jet, (b) Actual image of the subcooling jet behavior in the bulk liquid, (c) An illustration of expansion rate of the jet core in a radial direction.

and diameter of the droplet, 0.5 mm, respectively. In this study, we assume the shape of droplet is a sphere, then, $C_D = 0.47$ is applied. The jet has an unsteady behavior, and its velocity strongly depends on time. It is difficult to define the value of C_D under such situation, so here we applied the constant value for C_D. ρ_j and ρ_b in eq. (2) are densities of droplet and bulk liquid. Since the droplet temperature is lower than that of bulk liquid, ρ_j is large compared to ρ_b. The droplet velocity at Re = 1 is small because the diameter of droplet, d, is only 0.5 mm. For an example of a droplet at 25 °C which has ρ_j= 1680 kg/m^3 and μ_j = 0.00064 Pa·s, the velocity corresponding to Re = 1 is 0.762 mm/s. This means that the inertial resistance has a great influence on the motion of the droplet.

The gravitational force F_g of the subcooling droplet in the bulk liquid that is higher temperature compared by the droplet is

$$F_g = (\rho_j - \rho_b) V g, \tag{3}$$

where V is a volume of the droplet, $V = \pi d^3/6$. Therefore, equation (1) can be written

$$m\frac{dv}{dt} = \begin{cases} -C_D \frac{(\rho_j-\rho_b)Sv^2}{2} - (\rho_j - \rho_b) V g & \text{for } Re > 1, \\ -3\pi\mu d v - (\rho_j - \rho_b) V g & \text{for } Re < 1. \end{cases} \tag{4}$$

In the case of Re>1, velocity v and distance of x-direction x under the initial conditions of $v = v_0$ and $x = 0$ at $t = 0$ are

$$v = \sqrt{\frac{A}{B}} \tan\left\{ -t\sqrt{AB} + \tan^{-1}\left(v_0 \sqrt{\frac{A}{B}} \right) \right\}, \tag{5}$$

$$x = -\frac{\ln\left| \cos\left\{ -t\sqrt{AB} + \tan^{-1}\left(v_0\sqrt{\frac{A}{B}} \right) \right\} \right|}{A} - \frac{\ln\left| \cos\left\{ \tan^{-1}\left(v_0\sqrt{\frac{A}{B}} \right) \right\} \right|}{A}. \tag{6}$$

Similarly, v and x can be calculated for Re<1,

$$v = -\frac{B}{C} + \left(v_0 + \frac{B}{C} \right) \exp(-Ct), \tag{7}$$

$$x = -\frac{B}{C}t - \frac{\left(v_0 + \frac{B}{C}\right)\exp(-Ct)}{C} + \frac{v_0 + \frac{B}{C}}{C}, \tag{8}$$

where A, B and C in equations (5)∼(8) are

$$A = \frac{C_D(\rho_j - \rho_b)S}{2m},\ B = \frac{(\rho_j - \rho_b)Vg}{m},\ C = \frac{3\pi\mu d}{m}. \tag{9}$$

Now we consider that the subcooling jet expands in radial direction when the jet goes through the bulk liquid. In this experiment, the jet diameter is 1.5 times larger than initial diameter of the core part of the jet when the jet moves 48 mm in the x-direction as shown in **Fig. 4 (b)** and **(c)**. As mentioned before, inertial resistance has a large effect on the motion of the droplet, and here the effect of the expansion of the jet in the radial direction is applied to the resistance coefficient C_D. Therefore, we introduce the following modification to the inertial resistance coefficient C_D at an arbitrary position x,

$$C_D = C_D|_{x=0} \times \left(1 + \frac{0.5x}{0.048} \right) = 0.47 \left(1 + \frac{0.5x}{0.048} \right). \tag{10}$$

In this analysis model, it is note that the motion of droplet near the liquid surface in the tank is not discussed. The simple dynamic model here is estimated how high the subcooling jet rises in the bulk liquid. The motion of droplet including surface tension force at the liquid surface will be considered in the future.

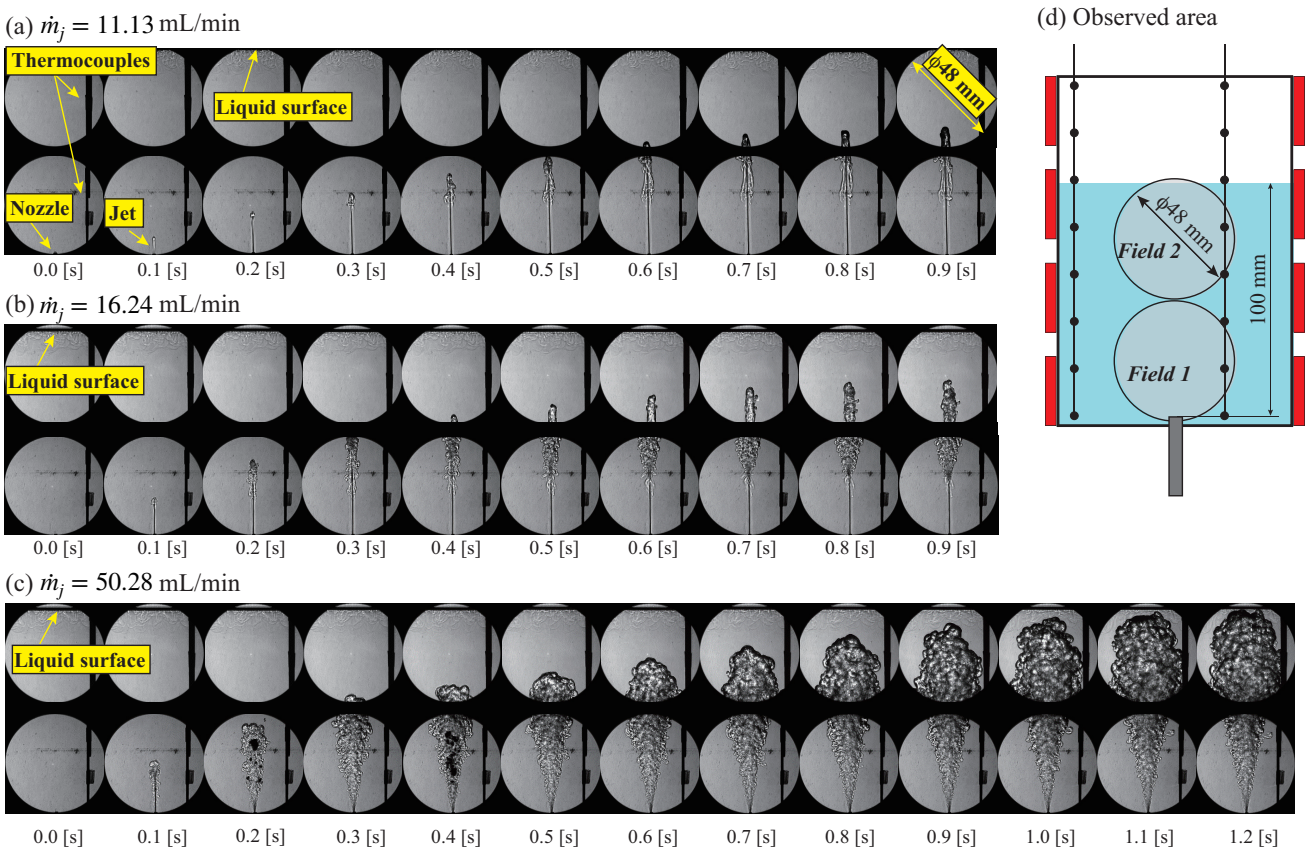

Fig. 5 Serial images of the subcooling jet motion taken by shadowgraph system. The flow rate of jet injected into bulk liquid in the test tank under various flow rate conditions; (a) $\dot{m}_j = 11.13$ mL/min, (b) $\dot{m}_j = 16.24$ mL/min, (c) $\dot{m}_j = 50.28$ mL/min. All the experiments are conducted at T_j = 19.2 °C, T_b = 33.3 °C, H_l = 100 mm. (d) Observation area of the shadowgraph system. The shadowgraph system has 48 mm in diameter as a field of view, and two field images of Field 1 and Field 2 were acquired in separate experiments under the same flow rate of subcooling jet.

4. Results and discussions

4.1 Ground experiment

Subcooling jet motion in the bulk liquid

Firstly, the comparisons between the results of the ground test and simple dynamic model discussed in the previous section are described. **Figure 5(a)∼(c)** shows the serial images of subcooling jet motion taken by shadowgraph system in ground. All the experiments are conducted at T_j = 19.2 °C, T_b = 33.3 °C, H_l = 100 mm. The flow rates of jet injected into bulk liquid in the test tank were carried out at (a) $\dot{m}_j = 11.13$ mL/min, (b) 16.24 mL/min, (c) 50.28 mL/min. The shadowgraph system has 48 mm in diameter as a field of view, and, as shown in **Fig. 5(d)**, two fields of view, "Field 1" and "Field 2", were acquired in separate experiments under the same experimental conditions. The images obtained from two separate experimental fields of view are synchronized by the starting time of injection of the jet. Therefore, note that the jet motions between the two fields are not completely synchronization but reasonably one.

The position of the tip of the jet was extracted from serial shadowgraph images **Fig. 5(a)∼(c)**, and the velocity and position in x-direction of the jet tip were plotted in **Fig. 6**. The position and velocity were derived from those images until the jet tip reached the highest position. In these figures, the experimental data between Filed 1 and Field 2 is in blank, because the data in this region cannot take by shadowgraph system. In addition, the results of the dynamic analysis model under the same conditions are also shown in **Fig. 6**. The initial velocities of the subcooling jet for each flow rate, v_0 were 0.945, 1.379 and 4.268 m/s in both model and experiment. In the early stage where the time is less than t = 0.2 sec, the velocity of the jet tip in the experimental data is slow and it tends to rise with time. This trend which is found only experimental data is due to unstable pump driving in the early stage. After that, the velocity gradually decreased, and the experimental data coincide with the results of analysis model. By contrast, the tip velocity of the jet in the early stage for dynamic analysis model is drastically slow down due to inertial resistance. Then, the velocity for dynamic analysis model gradually decreases and approaches a constant value, -5.663 mm/s, because viscous resistance and gravitational force are balanced finally.

The time variation of x-position of the tip of the jet in exper-

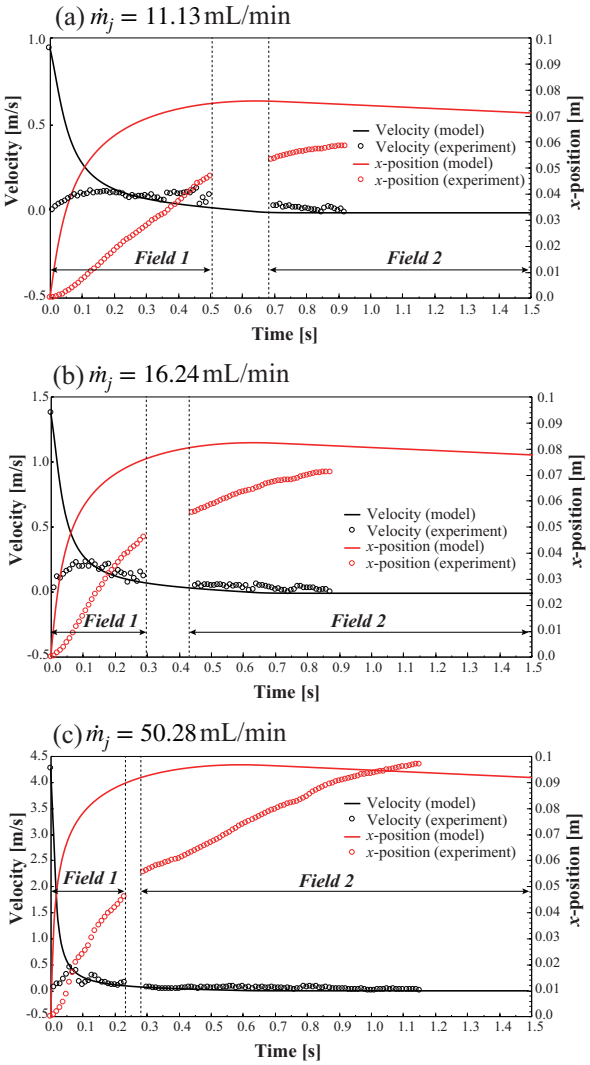

Fig. 6 Comparison of experimental data and analysis model for the velocity and x-position of the tip of jet. All conditions are same as Fig. 5(a), (b) and (c).

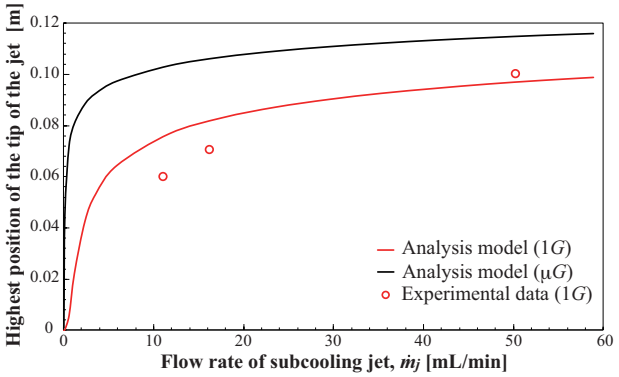

Fig. 7 Comparison of experimental data and analysis model for the highest position of the tip of jet. Three experimental conditions are same as Fig. 5(a), (b) and (c). The analysis model is calculated at at T_j = 19.2 °C, T_b = 33.3 °C. The gravitational acceleration in microgravity is set at 1×10^{-3} G.

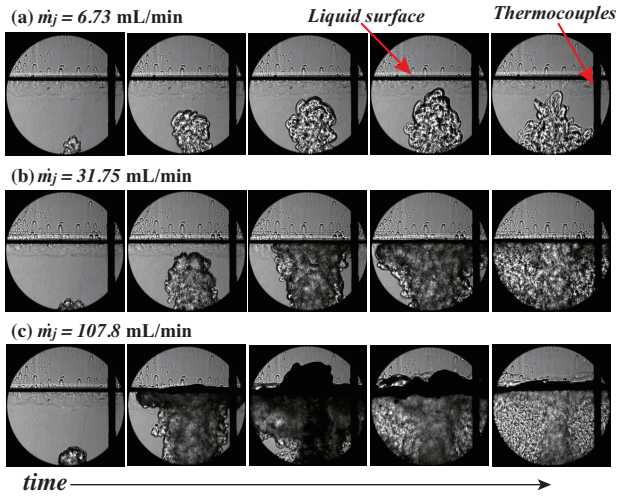

Fig. 8 Behavior of subcooling jet near the liquid surface at the flow rate (a) $\dot{m}_j$ = 6.73 mL/min, (c) $\dot{m}_j$ = 31.75 mL/min, (c) $\dot{m}_j$ = 107.8 mL/min. All the experiments are conducted at T_j = 14.0 °C, T_b = 28.6 °C, and H_l = 75 mm.

imental data is delayed compared with the analysis model. This delay is due to the velocity profile in the early stage. There is such a difference of time histories, however, the highest positions of the jet tip for the analysis model are roughly the same as the experimental data.

Figure 7 shows the highest position of the tip of the jet in the x-direction as a function of flow rate of the jet, $\dot{m}_j$. The results of analysis model both in ground and microgravity are also illustrated in this figure. Experimental values of maximum height as pointed by open symbols are low compared to analysis model, and its difference between them is larger with decreasing flow rate of the jet. However, these differences are not large, the differences are less than 1.2 cm. The analysis model is applied to the prediction of the maximum height of the jet in microgravity conditions (1×10^{-3} G), the height is approximately 2 cm higher than that in ground condition due to the gravitational force term is negligibly small.

Subcooling jet motion near the liquid surface

The one-dimensional simple dynamic analysis model described in previous section covers only the jet motion in the bulk liquid. Therefore, the surface tension acting on the jet at the liquid surface is not taken into consideration. Here, as an example, the behaviors of the subcooling jet near the liquid surface obtained by the shadowgraph images are explained. **Figure 8** shows the jet motion near the liquid surface at three different flow rates; (a) $\dot{m}_j$ = 6.73 mL/min, (c) 31.75 mL/min, (c) 107.8 mL/min. At a low jet flow rate as shown in **Fig. 8(a)**, the jet tip did not reach the liquid surface, however, in the case of moderate jet flow rate in **Fig. 8(b)**, the jet reached the liquid surface and then moved along the surface in the radial direction. Finally, the jet distributed

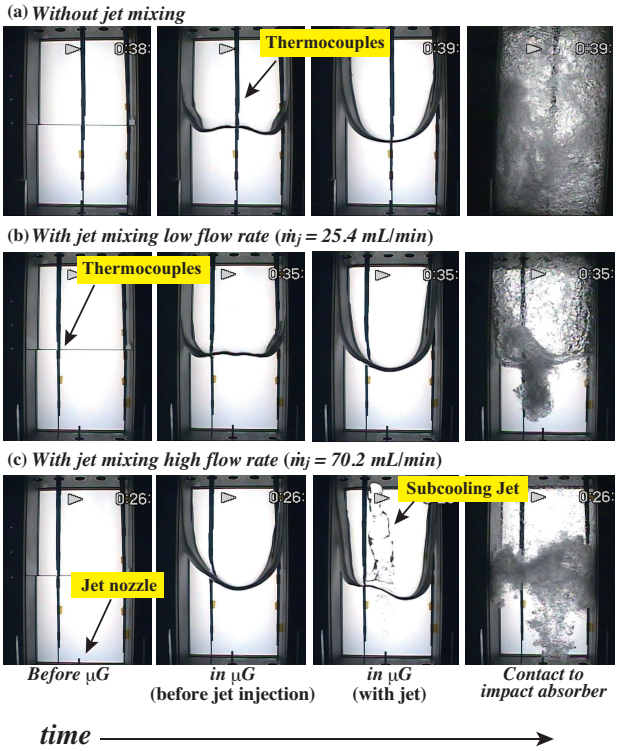

Fig. 9 Flow behavior in microgravity under the jet flow rate; (a) without jet injection, (b) $\dot{m}_j$ = 25.4 mL/min, (c) $\dot{m}_j$ = 70.2 mL/min. All the experiments are conducted at T_j = 16.2 °C, T_b = 30.2 °C, and H_l = 75 mm.

downward due to gravitational force. The liquid surface was unruffled and stabilized during jet injection at moderate flow rate. At a high flow rate of the jet as shown in **Fig. 8(c)**, the jet behavior was similar basically to the moderate flow rate except the motion of the liquid surface. The liquid surface was shaken violently, and formation of geyser was observed on the surface. These flow pattern were reported by Aydelott [17,18]. In order to explain these jet behaviors, the surface tension will be incorporated into the analysis model in the future study.

4.2 Microgravity experiment

Except for the CCD/Backlight system used as an observation method instead of the shadowgraph system, microgravity experiment was conducted with the same configuration as the ground experiment. The flow behavior in microgravity is shown in **Fig. 9**. Motion of subcooling jet in the bulk liquid could not observed by the CCD/Backlight observation system, however, the penetrating jet flow was found under high flow rate condition. The gravitational force term of the eq. (3) in the analysis model has not large effects for the jet behavior compared with the inertial resistance. In the high flow rate such as over 50 mL/min, the difference of highest position of the tip of subcooling jet between ground and microgravity conditions is smaller than 20 mm from the result of analysis model as shown in **Fig. 7**. In addition, the flow rate of the non-penetrating jet in the ground condition as shown in **Fig. 8(c)** is higher than highest flow rate in microgravity condition. Therefore, even in considering the effect of surface tension force at the liquid surface, it is hard to suppose that the subcooling jet penetrates the liquid surface under microgravity condition. It suggests that the penetrating jet flow in the **Fig. 9(c)** is caused by a flow in which the bulk liquid located just above the jet is pushed up due to the injection of the jet. To consider this issue, a microgravity experiment for observation of subcooling jet behavior with a shadowgraph system will be planned.

5. Conclusions

In order to estimate the motion of the tip of subcooling jet injected into the bulk liquid, the behavior of the jet by visualization method and description about the motion with a simple one-dimensional dynamic analysis model without heat transfer were reported in this study. We assumed a single sphere droplet as the tip of the jet in the model, and an equation of the motion was applied for the droplet. The results of analysis model and image data taken by shadowgraph system in ground experiment were compared. The trend of the tip velocity with time was well-matched excepting for the early stage where the time is less than t = 0.2 sec. And the highest positions of the tip for the analysis model were roughly the same as the experimental data.

From the microgravity experiment using the drop tower, unique flow behavior was observed. For more detailed study about jet behaviors, the surface tension will be incorporated into the analysis model and a microgravity experiment for observation of the subcooling jet behavior with a shadowgraph system will be carried out in the future study.

Acknowledgments

This research is carried out as a part of research project of the "Development of Innovative Thermal Management Technology to Realize Long-term Storage of Cryogenic Propellant" conducted in the Strategic Basic Development Research of the Space Engineering Committee in JAXA. Authors thanks to Mr. Kazuaki Nishida, who is a student of Muroran Institute of Technology, for his help for drop-tower experiment.

References

1) O. Kawanami: J. Jpn. Soc. Microgravity Appl., **18** (2001) 258.
2) D. J. Chato: Proc. of 43th AIAA Aerospace Sciences Meeting and Exhibit, Reno, Nevada, USA, January 2005, AIAA-2005-1148.
3) S. M. Motil and M. L. Meyer: Proc. of 45th AIAA Aerospace Sciences Meeting and Exhibit, Reno, Nevada, USA, January 2007, AIAA-2007-343.
4) M. Schaffer and C. Wenne: Proc. of Global pace Explo-ration Conference, Washington DC, USA, November 2012, GLEX-2012.05.1.4x12564.
5) D. W. Plachta: NASA/TM-1999-209389 (1999).
6) D. W. Plachta, J. Stephens, W. L. Johnson and M. Zagarola: Cryogenics, **94** (2018) 95.

7) L. J. Hastings, D. W. Plachta, L. Salerno and P. Kittel: Cryogenics, **41** (2001) 833.
8) X. W. Sun, Z. Y. Duo and W. Huang: Hydrogen Energy, **40** (2015) 9347.
9) D. W. Plachta, R. J. Christie, E. Carlberg and J. R. Feller: AIP Conference Proc., **985** (2008) 1475. DOI: 10.1063/1.2908506
10) W. U. Notardonato, A. M. Swanger, J. E. Fesmire, K. M. Jumper, W. Johnson and T. M. Tomsik: IOP Conf. Series: Materials Science and Engineering, **278** (2017) 012012.
11) S. H. Ho and M. M. Rahman: Hydrogen Energy, **40** (2012) 10196.
12) D. W. Plachta and M. C. Guzik: Cryogenics, **60** (2014) 62.
13) D. W. Plachta, W. L. Johnson and J. R. Feller: Cryogenics, **74** (2016) 88.
14) M. Kassemi and O. Kartuzova: Cryogenics, **74** (2016) 138.
15) M. Kassemi, O. Kartuzova and S. Hylton: Cryogenics, **89** (2018) 15.
16) M. Kassemi, S. Hylton and O. Kartuzova: P roc. of 2 018 Joint Propulsion Conference Cincinnati, Ohio, USA, July 2018, AIAA 2018-4940.
17) J. C. Aydelott: NASA Technical Paper 1487 (1979).
18) J. C. Aydelott: NASA Technical Paper 2107 (1983).
19) R. Imai, O. Kawanami, Y. Umemura and T. Himeno: IOP Conference Series: Materials Science and Engineering, **502** (2019) 012082.
20) J. G. Marchetta and R. H. Benedetti: Microgravity Science and Technology, **22** (2010) 7.
21) S. Barsi and M. Kassemi: J. of Thermal Science and Engineering Applications, **5** (2013) 041005. DOI: 10.1115/1.4023891
22) S. Barsi and M. Kassemi: J. of Thermal Science and Engineering Applications, **5** (2013) 041006. DOI: 10.1115/1.4023892